J. Mech. Phys. Solids 176 (2023) 105303

Contents lists available at ScienceDirect

Journal of the Mechanics and Physics of Solids

journal homepage: www.elsevier.com/locate/jmps

Hydrolytic crack growth and embrittlement in poly (ethylene terephthalate)

Atte Kadoma [1], Quan Jiao [1], Joost J. Vlassak [*], Zhigang Suo [*]

John A. Paulson School of Engineering and Applied Science, Harvard University, Cambridge, MA 02138, United States of America

ARTICLE INFO

Keywords:
Hydrolytic crack
Poly(ethylene terephthalate)
pH effect
Subcritical crack growth

ABSTRACT

Poly(ethylene terephthalate) (PET) is a thermoplastic of high-volume applications, and is identified as Number 1 in the Resin Identification Code on single-use packages. The ester bonds in the polymer chains are prone to hydrolysis, but the rate of hydrolysis is extremely low at room temperature. Here we show that hydrolysis causes PET to grow cracks even at room temperature and under low loads. The hydrolytic cracks greatly outrun erosion. When PET is submerged in water and subjected to a fixed load, the crack velocity increases with pH. At high loads, the crack grows rapidly, and hydrolysis is negligible, so that the crack grows with substantial plastic deformation and the fracture surface is rough. At low loads, the crack grows slowly and hydrolysis is fast enough, so that the crack grows with negligible plastic deformation and the fracture surface is smooth. These observations show that hydrolysis embrittles PET. Under development for sustainability and healthcare are biodegradable and biomass-derived polymers, many of which have hydrolysable groups in the main chains or crosslinks. They are all potentially susceptible to hydrolytic crack growth and embrittlement. It is hoped that this study will aid the development and applications of these polymers.

1. Introduction

Poly(ethylene) terephthalate (PET) has high-volume applications due to its strength, transparency, dimensional stability, and low permeability to gasses (Nisticò, 2020). Ubiquitous uses include beverage bottles and food containers (The future of plasic, 2018). PET fibers, known as polyester fibers in the textile industry, have low moisture absorbency, high shrink resistance, and high wear resistance (Militky, 2009). Blends of PET and natural fibers are used in upholstery filling and sportswear (Kothari et al., 2008). The durability of PET creates problems at the end of its use. Despite decades of effort in the development of recycling, post-consumer PET is primarily landfilled (Geyer et al., 2017; Ragaert et al., 2017). A landfilled PET bottle is estimated to last over a millenia (Chamas et al., 2020). Even for multi-use applications, such as clothes, microplastics created during wear and wash make their way into the waste stream, the environment, and then the food chain (De Falco et al., 2019; Hunt et al., 2021; Lim, 2021). Under investigation are sustainable ways to salvage post-consumer PET. For example, recycled PET fibers have been considered to reinforce concrete (Gu and Ozbakkaloglu, 2016).

The degradation of PET has long been studied (Amborski and Flierl, 1953; Buxbaum, 1968; Golike and Lasoski, 1960; McMahon et al., 1959; Ravens, 1960). PET degrades by hydrolysis, in which an ester bond in a PET chain is broken by reacting with an active

* Corresponding authors.
E-mail addresses: vlassak@seas.harvard.edu (J.J. Vlassak), suo@seas.harvard.edu (Z. Suo).
[1] These authors equally contributed to this work.

https://doi.org/10.1016/j.jmps.2023.105303
Received 13 February 2023; Received in revised form 8 April 2023; Accepted 20 April 2023
Available online 25 April 2023

species, such as a water molecule or a hydroxyl ion in the environment (Nisticò, 2020). The rate of hydrolysis is appreciable at elevated temperature, but negligible at room temperature (Golike and Lasoski, 1960). The claim that hydrolysis of PET is negligible at room temperature, however, must be re-evaluated in light of recent findings in another thermoplastic polyester: poly(lactic) acid (PLA). When a PLA sample is subject to even a small load, general erosion is greatly outrun by a hydrolytic crack (Yang et al., 2021). Furthermore, PLA suffers from hydrolytic embrittlement at room temperature (Shi et al., 2022).

The discovery of hydrolytic crack growth dates back to Orowan (Orowan, 1944). Silica glass can sustain a low force for a long time, and then suddenly fracture. Orowan attributed such delayed fracture not to viscoelasticity, but to hydrolysis at a crack tip. Wiederhorn (1967, 1968) presented systematic studies on hydrolytic crack growth of silica glass. It was found that the crack velocity is a function of relative humidity and energy release rate. Similar environmentally assisted crack growth has been reported in other materials, and has raised concerns in load-bearing applications. A well-known example is ozone cracking in natural rubber (Braden and Gent, 1960). The unsaturated carbon bonds in polymer chains are oxidized by ozone, causing crack growth at small strains. This phenomenon has been widely observed in products such as tires, fuel lines, and rubber seals. Ozone cracking is addressed by antioxidant additives (Braden and Gent, 1960). A recent study shows that during rainstorms particles worn off the tires are washed into rivers, where antioxidants leach out and kill fish (Tian et al., 2021). We have reported environmentally assisted crack growth in several polymers with hydrolysable bonds, including poly(glycerol sebacate) (Shi et al., 2020), poly(dimethylsiloxane) (Jiao et al., 2021; Yang et al., 2019), and poly(lactic) acid (Shi et al., 2022). In the absence of hydrolysis, these polymers have high toughness. However, in a humid environment, such polymers grow cracks even under a small load.

In the absence of hydrolysis, a polymer with hydrolysable bonds can undergo general erosion (Fig. 1a). However, in a humid environment and under a small external load, such a polymer is vulnerable to cracks which greatly outrun erosion (Fig. 1b). Here we investigate if hydrolytic crack growth takes place in PET. We submerge a PET film with a precut in water, subject the film to a fixed load, and measure the velocity of the crack. To accelerate crack growth, PET is submerged in an aqueous solution of a high pH. At a low load, the crack grows slowly, and hydrolysis is fast enough to cause chain scission, so that the crack grows with negligible chain slip. At a high load, the crack grows rapidly, and hydrolysis is too slow to cause chain scission, so that the crack grows with extensive chain slip. That is, PET suffers from hydrolytic embrittlement. The fracture surface is smooth when the crack grows slowly and chain scission dominates, but is rough when the crack grows rapidly and chain slip dominates. We further show that, under a fixed load, the hydrolytic crack grows rapidly at a high pH, but grows negligibly at a low pH. Although hydrolytic erosion of PET has been known for a long time, hydrolytic crack growth in PET has not been reported before. This finding is directly relevant to the development of sustainable uses of post-consumer PET. Furthermore, many biodegradable polymers and biomass-derived polymers have hydrolysable groups in the main chains, making these polymers also vulnerable to hydrolytic crack growth. It is hoped that this study will aid the development and applications of these polymers.

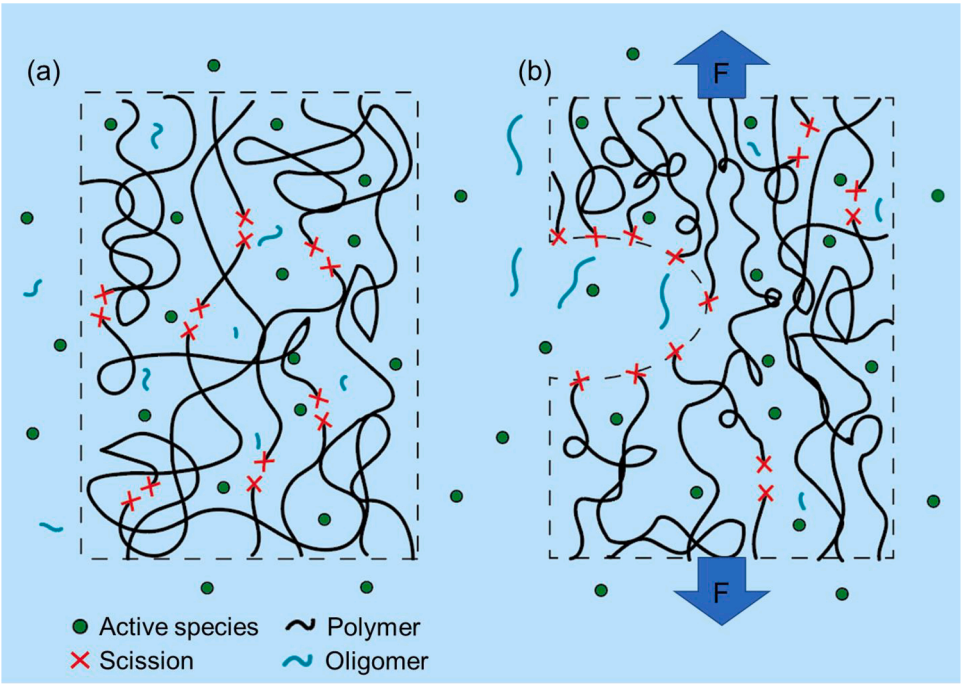

Fig. 1. Hydrolytic erosion vs. hydrolytic crack growth. A PET sample is submerged in an aqueous solution. The ester bonds in the polymer chains can break when reacted with water molecules or active species in the solution. (a) In hydrolytic erosion, in the absence of applied force, broken segments of the polymer transfer from the PET sample to the solution. (b) In the presence of an applied force, polymer chains break preferentially near a crack tip, and the crack grows.

2. Materials and methods

PET film with a thickness of 50 μm was purchased from McMaster-Carr (product #8567K22). McMaster-Carr describes this product as comparable to Dupont Mylar® and Melinex®, which are known to be processed by biaxial stretching. The manufacturer specified thickness of the specimen was verified with a digital thickness gauge (Neoteck, NTKTL495-US). As the PET film is a commercial material, details on composition and processing are unavailable to us. Thus, we conducted several characterization tests.

The PET was characterized by differential scanning calorimetry (TA Discover 250). A 4.32 mg mass of PET film was placed in the calorimeter, heated from 25°C to 300°C at a rate of 10°C/min, and then cooled at the same rate to 25°C.

The PET was also characterized by uniaxial tension tests in two directions, along and transverse to the rolling direction of the film. Dog-bone shaped samples of width 2 mm and gauge length 12 mm were cut in each orientation per ISO 527-2-5B standard using a cutting die (Ace Steel Rule Dies). A tensile tester (Instron 5966) applied displacement at a constant rate of 0.1 mm/s to the samples, while the force was recorded at a frequency of 20 Hz. Stress is calculated as the force divided by the cross-sectional area of the undeformed sample. Strain is calculated as the elongation divided by the gauge length of the undeformed sample. Six samples of each orientation are tested.

Toughness of the polymer film in the two orientations was measured by 180° tear. Rectangular samples were cut in dimensions 100 mm by 50 mm. A 10 mm precut was introduced by a scissor, which bisected the width of the film, and the width of each arm was $B = 25$ mm. One arm was clamped by the top gripper of the tensile tester, and the other arm was clamped by the bottom gripper. The two arms formed an angle of 180°. The tensile tester pulled the top arm at a constant velocity of 0.1 mm/s relative to the bottom arm, and the force was recorded at a frequency of 20 Hz.

A chamber was assembled to study hydrolytic crack growth in PET film by 90° tear (Fig. 2). A styrene methyl methacrylate container was covered with a removable acrylic lid. Two L-shaped acrylic brackets were fixed to the lid to form a shelf. The components of the chamber were optically transparent, so that the growth of the crack could be recorded by a digital microscope (Celestron, 5 MP Handheld Digital Microscope Pro), which was placed on top of the chamber. Precut specimens were prepared in the same dimensions as those for the measurement of toughness. One arm of the film was glued to an acrylic substrate with cyanoacrylate (Krazy Glue), and the other arm of the film was vertically loaded with a hanging mass (2 g to 45 g). The acrylic substrate was placed onto the shelf, which was then lowered into the chamber. The sample was then submerged in a buffered aqueous solution. Buffered solutions were chosen to ensure the pH remained within ± 0.1 throughout the duration of all experiments. We prepared various buffered solutions of pH = 1, 3, 7, 9, 11, and 13 by mixing hydrochloric acid or sodium hydroxide solution, salt solution B, and deionized (DI) water (Table 1). The solutions were monitored using a pH meter (Aperta Instruments PH60). Hydrochloric acid (HX0603-3), potassium hydrogen phthalate (product #1024000080), and potassium phosphate monobasic (product #5655) were purchased from Millipore Sigma. Potassium chloride (product #6858) was purchased from Mallinckrodt, and Sodium Hydroxide (S8045) was purchased from Sigma-Aldrich.

Scanning electron microscopy imaging was conducted on fractured specimens. Tested samples were gently rinsed with deionized water and dried in air. To prevent charging, the samples were coated with 5 nm-thick $Pt_{80}Pd_{20}$ alloy using a sputter coater (EMS 150T S metal sputter coater). The fracture surfaces were imaged (Zeiss Ultra Plus) at an accelerating voltage of 3 kV.

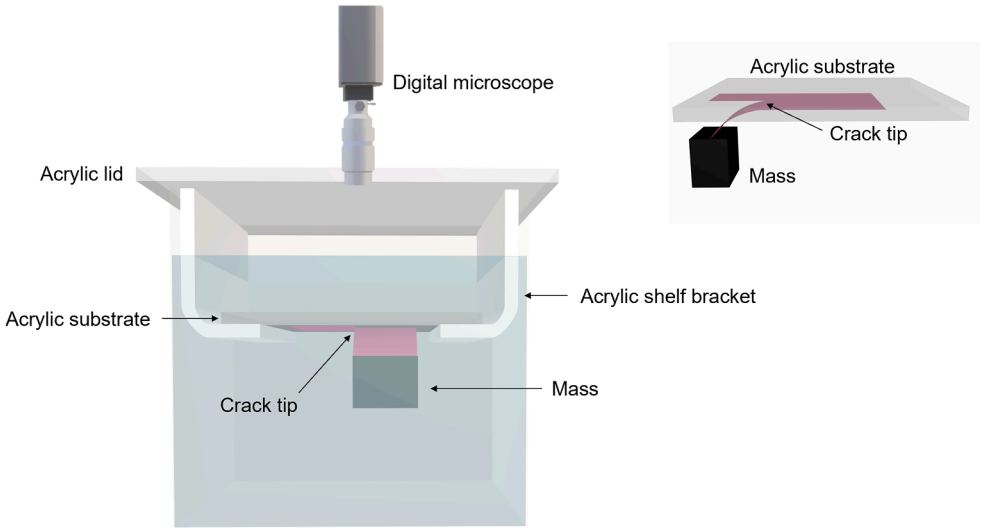

Fig 2. Schematic of an experimental setup for the study of hydrolytic crack growth. One arm of a PET film is glued to an acrylic substrate, and the other arm is attached to a hanging mass. The substrate is placed on an acrylic shelf in a chamber, so that the sample is submerged in an aqueous solution. Crack growth is recorded by a digital microscope.

Table 1
Recipes for the preparation of buffered aqueous solutions. Each buffered solution is prepared by mixing the indicated volumes of A and B with DI water to form a 100 mL solution.

	A: acid/alkali solution		B: salt solution	
pH =1	0.2 M HCl	67 mL	0.2 M KCl	25 mL
pH = 3	0.1 M HCl	22.3 mL	0.1 M $C_8H_5KO_4$	50 mL
pH = 7	0.1 M NaOH	29.1 mL	0.1 M KH_2PO_4	50 mL
pH = 9	0.1 M NaOH	4.4 mL	0.1 M $C_2H_5NO_2$	25 mL
pH = 11	0.1 M NaOH	4.1 mL	0.05 M Na_2HPO_4	50 mL
pH = 13	0.2 M NaOH	66 mL	0.2 M KCl	25 mL

3. Results

Differential scanning calorimetry (DSC) is commonly used to characterize polymers. DSC scans of an as-received PET film are plotted as a function of temperature (Fig. 3). The vertical axis is the flow of energy per unit time and per unit mass to or from the sample. This axis is taken to be positive when the enthalpy of the sample increases. The area under the curve divided by the rate of temperature change gives the increase in enthalpy. PET is a semicrystalline polymer. When the temperature is increased, the amorphous regions within the sample undergo a transition from the glassy phase to the rubbery phase, as seen by a small perturbation of the heating curve. The crystalline regions melt at 243°C, as shown by a significant increase in the rate of energy flow. When the temperature is decreased, the sample crystallizes at 211°C, as shown by a substantial decrease in the rate of energy flow. As the temperature reduces further, the amorphous regions undergo a transition from the rubbery phase to the glassy phase at 76°C. Commercial polymers can be characterized by melting temperature and glass transition temperature. For example, PET has a melting temperature of 255 - 267°C and a glass transition temperature of 67 - 81°C (Nisticò, 2020; Robertson, 2016; Ronkvist et al., 2010). Our measurements by DSC are comparable to the values reported in the literature, which confirms that the purchased McMaster-Carr product is PET.

The crystallinity is estimated by

$$X = \frac{\Delta H_m}{\Delta H_{m^\circ}}$$

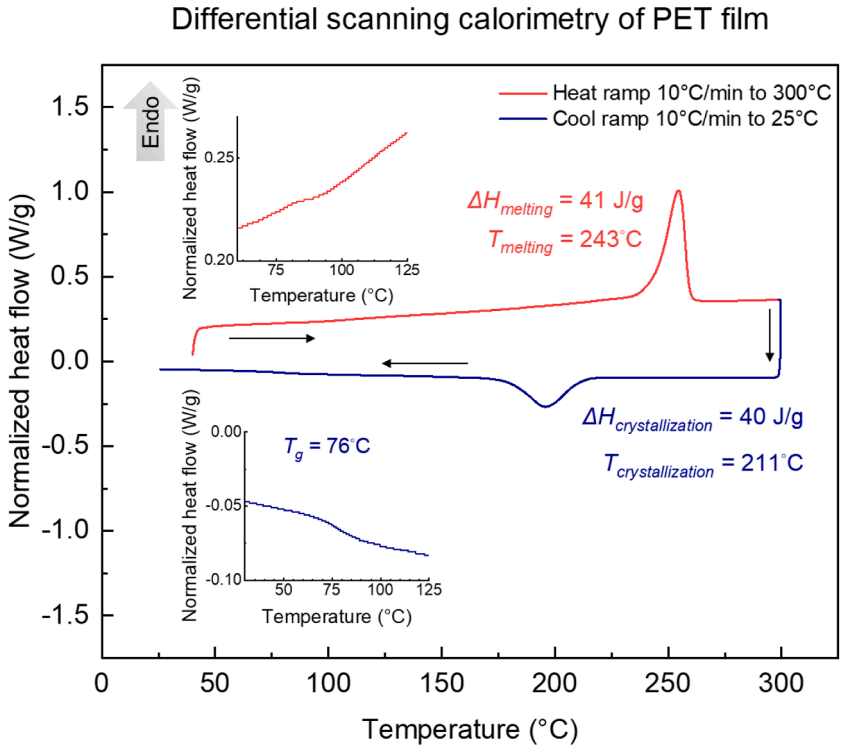

Fig. 3. Differential scanning calorimetry (DSC) measurement of as-received PET film. The temperature of the sample is increased at a rate of 10°C/min, and is then decreased at the same rate. The rate of energy flow is taken to be positive when the sample gains enthalpy. The two insets magnify parts of the curves where the sample undergoes the glass-to-rubber and rubber-to-glass transitions.

where ΔH_m is the specific enthalpy of melting obtained in the DSC measurement, and ΔH_{m° is the specific enthalpy of melting of crystalline PET. We adopt $\Delta H_{m^\circ} = 140$ J/g (Ronkay et al., 2020). Integrating the flow of energy from the onset of melting to the end of melting and dividing by the rate of temperature change, we obtain $\Delta H_m = 41$ J/g. Consequently, the as-received film is 29% crystalline. Similarly from the cooling curve, we obtain $\Delta H_m = 40$ J/g. Consequently, the sample after one cycle of heating and cooling is still about 29% crystalline.

Our measured crystallinity is close to that commonly reported for biaxially oriented PET. A biaxially oriented PET is stretched in a two step process (Robertson, 2016). A crystallinity of 10 -14% is induced by stretching the film in a machine oriented direction. The film is then stretched transverse to the machine oriented direction, thereby increasing the crystallinity to 20 - 25%. The film is then

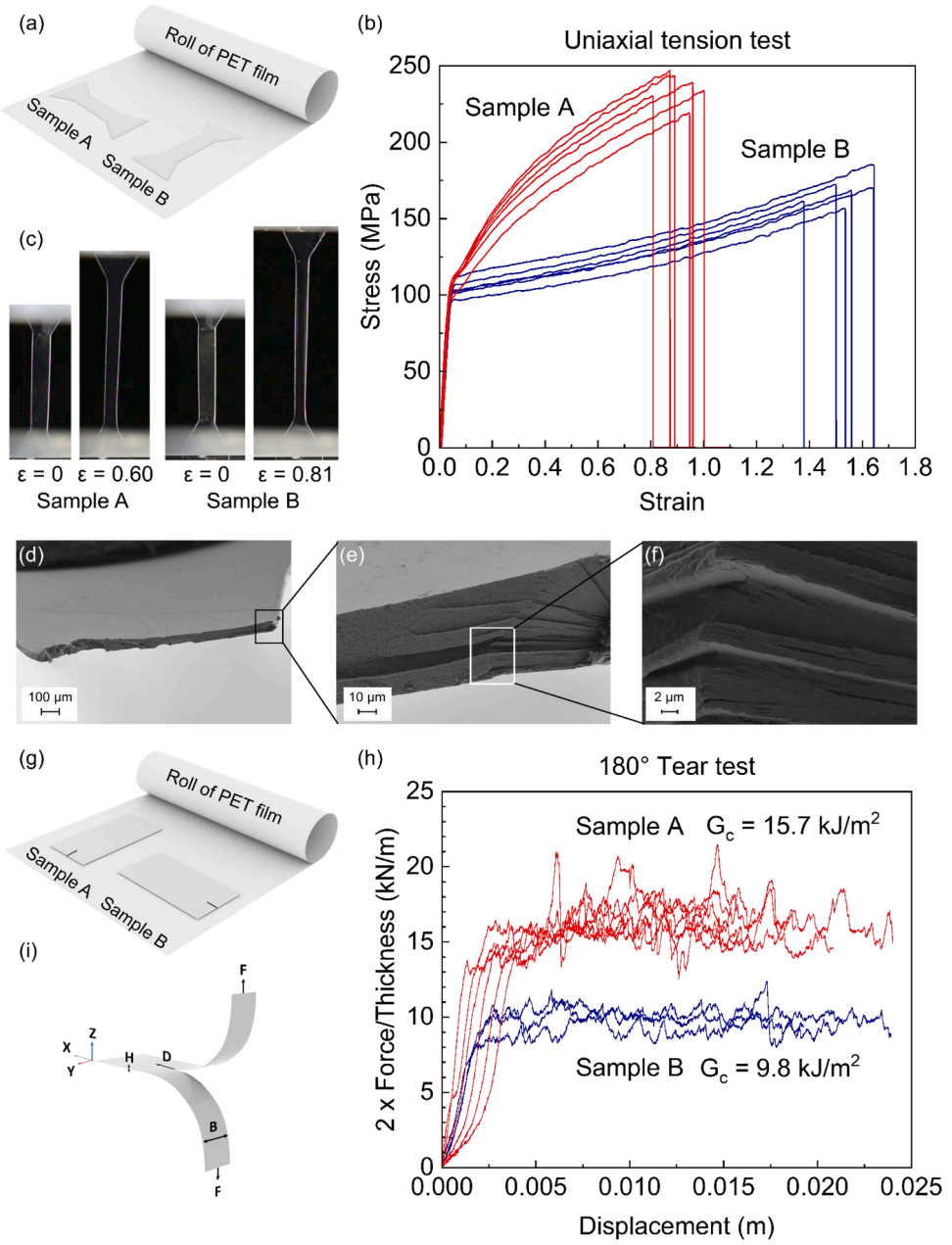

Fig. 4. Mechanical Tests. (a) Dogbone-shaped tensile samples are cut in two orientations: A (crack runs in the rolling direction of the film), and B (crack runs in the direction transverse to the rolling direction of the film). (b) Stress-strain curves of the samples of the two orientations. (c) Photographs of the samples in the undeformed state and deformed state. (d)-(f) Scanning electron microscopy images of several magnifications of a fracture surface of a crack running transverse to the rolling direction (sample of orientation B). (g) Fracture samples are cut in two orientations from a roll of film. (h) The force-displacement curves for samples of the two orientations. (i) Schematic of 180° tear.

annealed while constrained which can increase the percent crystallinity up to 40%. It is known that crystallinity affects the rate of hydrolysis (Allen et al., 1994; Golike and Lasoski, 1960; Hosseini et al., 2007; Kaabel et al., 2021). This effect, however, is not studied in this paper.

We conduct uniaxial tensile tests on dogbone-shaped samples cut in two orientations from the as-received film (Fig. 4a). As the tensile tester pulls a sample, the sample deforms elastically, yields, strain-hardens, and fractures (Fig. 4b). All samples deform uniformly and remain transparent throughout the test (Fig. 4c). When a sample fractures under uniaxial tension, the fracture surface does not show substantial localized plastic tearing (Fig. 4d). A high-resolution image shows that some region of the fracture surface has a laminar structure (Fig. 4e). Similar laminar structures have been reported before for biaxially processed thermoplastic films (Lu et al., 2018; Rytöluoto et al., 2017; Shayanipour and Bagheri, 2019). It appears that after homogeneous plastic deformation, the sample fractures in a brittle manner (Fig. 4f). We characterize the stress-strain curve of a tensile test by six properties: modulus, yield strength, yield strain, fracture strength, fracture strain, and work of fracture. We obtain the work of fracture by integrating the area underneath the stress-strain curve.

We measure the toughness of the PET film using 180° tear. Samples are cut from the as-received film in two orientations (Fig. 4g). As the two arms of a sample are pulled by the tensile tester at a constant velocity, the crack advances (Fig. 4i). The machine records the force-displacement curve (Fig. 4h). When the displacement is small, the force increases with the displacement, and the crack does not advance. When the displacement exceeds a critical value, the force plateaus, and the crack advances steadily. Recall the energy release rate for a tear test (Jia et al., 2022; Rivlin and Thomas, 1953):

$$G = \frac{2F(\varepsilon+1)}{H} - 2BW$$

where F is the plateau force, ε is the strain in the arm, H is the thickness of the arm, B is the width of the arm, and W is the elastic energy density at steady-state crack growth. The plateau force is on the order of $F \sim 4$ N, and the width and thickness of the film are $B = 25$ mm and $H = 50$ μm, respectively. Consequently, the nominal stress in the arm is $F/HB = 3.2$ MPa. We have measured the stress-strain curve of the PET (Fig. 4b). At this stress level, the PET is in the elastic regime, and the strain is small, $\varepsilon \sim 0.1\%$. Under the conditions that $\varepsilon << 1$, W is much smaller than the nominal stress F/HB, so that the above equation reduces to $G = 2F/H$. The tear test is repeated five times for cracks running along the rolling direction of the film (orientation A), and three times for cracks running transverse to the rolling direction (orientation B).

The seven properties are listed for samples in which fracture runs transverse to and along the rolling direction of the film (Tables 2 and 3). We compare average properties of samples in the two orientations. Samples of orientation A have a somewhat higher modulus than samples of orientation B. We interpret this observation as an indication that polymer chains are slightly more oriented along the transverse direction of the film. Samples of the two orientations have comparable yield strength and yield strain. Samples A strain-harden more steeply and have a higher fracture strength than samples B. Samples A have a lower fracture strain and work of fracture, but a higher toughness, than samples B.

Tables 2 and 3 also list the standard deviation and coefficient of variation (COV) of each property. The COV of a property is defined by dividing the standard deviation by the average, and gives a dimensionless measure of the dispersion of the property. The standard deviation of each property has its own unit, so it cannot be compared to that of another property. By contrast, COV is a dimensionless measure of sample dispersion, which allows us to compare COVs of various properties. Observe that the COV for every property of sample in each orientation is smaller than 25%. In particular, the fracture strength, fracture strain, and work of fracture have comparable COVs to those of the modulus and toughness. These observations of PET may be contrasted with those of a brittle material such as silica glass. In silica, modulus and toughness have small statistical variations, but fracture strength and fracture strain can vary by orders of magnitude from sample to sample (Griffith and Taylor, 1921; Proctor et al., 1997). Such behavior of silica glass is commonly understood as follows. Fracture strength and fracture strain are sensitive to flaws, but modulus and toughness are not. We interpret our observations of PET to be typical of a ductile material, in which all the seven properties are insensitive to flaws.

The work of fracture, W_c, measured by performing a tensile test on a sample without precut, is the energy per unit volume required to fracture the bulk of a material. The toughness, G_c, measured by performing a tear test on a sample with precut, is the energy per unit area required to advance a crack. The ratio of these two material properties defines yet another material property: the fractocohesive length, G_c/W_c (Chen et al., 2017). A material may contain flaws of various sizes. When the flaws are smaller than the fractocohesive length, the material fractures at a strength independent of the flaw size. On the other hand, when the flaws are larger than the fractocohesive length, the material fractures at a strength that decreases as the flaw size increases (Chen et al., 2017).

The average fractocohesive length of PET is 98 μm for samples A and 49 μm for samples B. Chen and coauthors have collected the fractocohesive lengths for various metals, ceramics, and polymers (Chen et al., 2017). Silica glass has a fractocohesive length of 1 nm. The strength of silica glass is extremely sensitive to flaws. Any flaw ranging in size from an atomic-scale flaw to a macroscopic scratch will reduce the strength of silica. Consequently, silica has a large statistical variation in fracture strength (Griffith and Taylor, 1921;

Table 2
Properties of samples when fracture runs in the rolling direction of the film (orientation A).

	Modulus	Yield strength	Yield strain	Fracture strength	Fracture strain	Work of fracture	Toughness
Average	3.5 GPa	100 MPa	4%	240 MPa	90%	160 MJ/m^3	15,700 J/m^2
Standard deviation	0.3 GPa	7 MPa	1%	9 MPa	6%	10 MJ/m^3	500 J/m^2
Coefficient of variation	8.6%	7.1%	25.0%	3.8%	6.6%	7.8%	3.2%

Table 3
Properties of samples when fracture runs in the direction transverse to the rolling direction of the film (orientation B).

	Modulus	Yield strength	Yield strain	Fracture strength	Fracture strain	Work of fracture	Toughness
Average	2.9 GPa	90 MPa	4%	160 MPa	150%	200 MJ/m^3	9,800 J/m^2
Standard deviation	0.5 GPa	10 MPa	1%	10 MPa	9%	20 MJ/m^3	600 J/m^2
Coefficient of variation	17.2%	10.1%	25.0%	6.1%	5.8%	10.6%	6.1%

Proctor et al., 1997). Natural rubbers have a fractocohesive length of 1 mm (Chen et al., 2017). The strength of natural rubber is insensitive to microscopic flaws, but is sensitive to macroscopic flaws. The fractocohesive length of PET is on the order of 100 μm. Consequently, we observe small statistical variation in the fracture strength of this material (Fig. 4b), as well as a modest coefficient of variation (Tables 2 and 3).

We study hydrolytic crack growth in solutions of pH = 1, 3, 7, 11, and 13 at a constant energy release rate (Fig. 5a). Hydrolytic crack growth is tested by 90 degree tear, and the energy release rate is calculated by $G = F/H$. We choose to limit our study to cracks running in the direction transverse to the rolling direction of the film (i.e., the direction with a lower toughness, sample of orientation B). The toughness in this direction is $G_c \approx 9{,}800$ J/m^2. To prevent sudden uninhibited crack propagation, we load the specimens to an energy release rate of $G = 4{,}400$ J/m^2. The crack velocity has strong dependence on the pH of the solution (Fig. 5a). There is significant hydrolytic crack growth in basic solutions. Crack velocity increases by about four orders of magnitude from pH = 9 to pH = 13. On the other hand, we do not observe crack growth in neutral and acidic solutions within the resolution and time of the experiments. To estimate an upper-bound velocity, we divide the resolution of the distance measurement in our setup (i.e., 100 μm) by the duration of the experiment (14 days), and plot a downward arrow for each experiment in which no crack extension is observed.

We also study hydrolytic crack growth in a high-alkaline solution, pH = 13, under various loads (Fig. 5b). From $G = 350$ to $G = 1{,}000$ J/m^2, the crack velocity increases sharply with energy release rate. Next, from $G = 1{,}000$ J/m^2 to $G = 7{,}000$ J/m^2, crack velocity increases much slower than the initial regime. Finally, as the energy release rate approaches the toughness of the material, we see another sharp increase in crack velocity.

At a low energy release rate, $G = 350$ J/m^2, the crack grows at a velocity of 10^{-7} m/s and the fracture surface shows negligible plastic deformation (Fig. 5c). Occasionally layers of material are pulled out in the middle of the surface, indicating some plastic deformation. At a high energy release rate, $G = 5{,}200$ J/m^2, the crack grows at a velocity of 5×10^{-6} m/s and the fracture surface shows extensive plastic deformation (Fig. 5d). Layers of PET are pulled out of the material. Surface morphology is not altered with

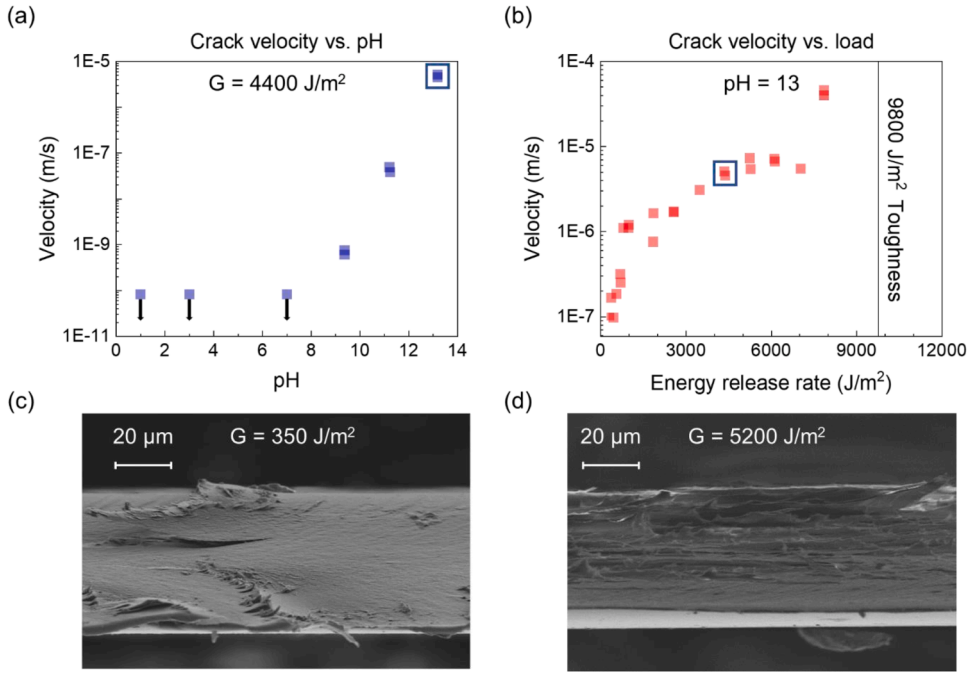

Fig 5. Hydrolytic crack growth. (a) Crack velocity as a function of pH at an energy release rate of 4,400 J/m^2. Each data point represents an observed crack velocity. Each arrow represents a stationary crack within the resolution of length (100 μm) and time of observation (14 days). Data points in the blue square are common to Fig. 5a and 5b. (b) Crack velocity as a function of energy release rate for samples in a solution of pH = 13. (c) At $G = 350$ J/m^2, the crack surface is smooth with negligible plastic deformation. (d) At $G = 5{,}200$ J/m^2, the crack surface shows extensive plastic deformation. In both cases, the cracks propagate from left to right.

further increases in energy release rate. Fracture occurs by chain scission, chain sliding, or a combination of the two processes near the crack tip, depending on energy release rate. At a low G, the crack grows slowly enough for hydrolysis to take place, and the crack grows primarily by chain scission with negligible chain slip: the fracture is brittle. At a high G, the crack grows too fast for hydrolysis to take place, and the crack grows with extensive chain slip and some chain scission: the fracture is ductile. As energy release rate is increased, fracture undergoes a brittle-to-ductile transition.

4. Discussion

4.1. Reaction of polyester in aqueous solution

Hydrolysis of ester bonds has been extensively studied (Jung et al., 2006). In a low pH environment, a hydronium ion (H_3O^+) catalyzes the reaction between a water molecule and an ester bond (Fig. 6a), producing one molecule terminated by a carboxylic acid and another molecule terminated by an alcohol group. This process is called acid-catalyzed hydrolysis. In a high pH environment, a hydroxyl ion (OH^-) directly reacts with an ester bond in an aqueous environment to produce a molecule terminated by a carboxylate group and a molecule terminated by an alcohol group (Fig. 6b). This process is called base-catalyzed hydrolysis.

It is known that, for ester bonds, acid-catalyzed hydrolysis is much slower than base-catalyzed hydrolysis. This trend also applies to PET and has been characterized in different types of experiments. Amborski and Flierl (Amborski and Flierl, 1953) showed tear strength and tensile strength decrease significantly for PET submerged in basic solutions, but much less so in acidic solutions. Measurements of the viscosity of PET chains in a solvent also indicate that hydrolysis is slower in acidic solutions than basic solutions, although the rate of hydrolysis starts to increase at a pH less than zero (Ravens, 1960). At neutral pH, many studies show that PET undergoes negligible hydrolysis below the glass transition temperature (Golike and Lasoski, 1960; McMahon et al., 1959). Unfortunately, we cannot make a quantitative comparison between the crack velocity and chemical reaction due to the data unavailability on the rate of hydrolysis at different pH. Nevertheless, our own observations that hydrolytic crack grows in basic solutions, but negligibly in neutral and acidic solutions is consistent with the above observations.

Furthermore, we note that the hydrolytic crack growth experiment conducted in this paper should not be compared to a previous measurement of tear strength (Amborski and Flierl, 1953). These authors measured tear strength after a sample was submerged in an aqueous solution for some time. They did not measure crack velocity while the sample was submerged in an aqueous environment. Consequently, their experiment characterized general degradation (Fig. 1a), which is different from hydrolytic crack growth (Fig. 1 (b)).

4.2. Crack outruns erosion

As illustrated in Fig. 1, hydrolysis of a polymer can cause both erosion and crack growth. At a high pH, we observe that a crack outruns erosion. The crack grows centimeters in a couple of days without noticeable change in the external dimensions of the sample. We interpret this observation as follows.

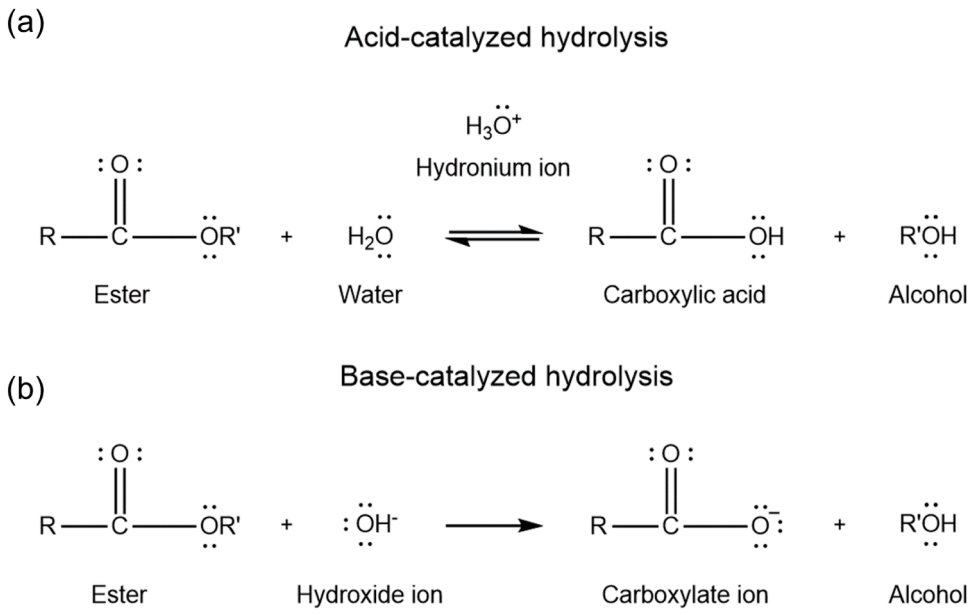

Fig 6. Hydrolysis of an ester bond in an aqueous environment. (a) Hydrolysis in an aqueous solution of low pH. (b) Hydrolysis in an aqueous solution of high pH.

For the sample to erode, ester bonds must be broken into oligomers, which are then dissolved into the surrounding solution (Göpferich, 1996; Sevim and Pan, 2018). If the reaction is fast, reactants diffuse slowly, and the sample is large, chain scission mainly takes place at the sample surface. If the reaction is slow, reactants diffuse fast, and the sample is small, chain scission takes place throughout the bulk. When a long polymer chain near the surface of a thermoplastic is broken by hydrolysis of a few ester bonds, the broken chains, so long as they are not too short, remain attached to the sample by the same interchain interactions that bind the thermoplastic polymer. That is, the debris of broken polymer chains remains attached to the sample and slows down the transport of reactive species from the surrounding solution to the interior of the sample. By contrast, a crack provides a path for the reactive species from the surrounding solution to reach the crack tip. The crack advances when hydrolysis breaks polymer chains at the surface of the crack tip or in a small volume around the crack tip. Compared to erosion, the advancing crack shortens the path for the transport of the active species in the polymer.

Hydrolytic crack growth in polymers has received attention recently, and its mechanism is still under investigation (Baumberger, 2022; Shi et al., 2022; Yang et al., 2019, 2021). Hydrolysis can break polymer chains either at the surface or in the bulk of a sample (Burkersroda et al., 2002). Because a crack outruns surface erosion, here we focus on hydrolysis at the surface, or in a small volume around the crack tip. For crack growth by hydrolysis at the surface of the crack tip, the velocity of the crack may be limited either by the reaction or by the transport of the reactive species in the surrounding solution. For crack growth by hydrolysis in a small volume around the crack tip, the crack velocity may be further limited by transport of the reactants in the polymer. In either case, the applied load may also accelerate crack growth by lowering the activation barrier of the reaction by the stress concentrated around the crack tip. To sort out these mechanisms of hydrolytic crack growth, further experiments are needed.

4.3. Potential experiments to study rate-limiting processes for hydrolytic crack growth in PET

Crack velocity depends on energy release rate, chemical environment, temperature, and the microstructure of PET. By changing these conditions, mechanisms of hydrolytic crack growth in PET can be probed. In this paper, we have only varied energy release rate and pH. In subsequent work, we hope to observe crack velocity at even lower values of energy release rate, which will further reduce the effect of plastic deformation and help to differentiate hydrolytic crack growth by stress-assisted hydrolysis and transport-limited hydrolysis.

We plan to observe hydrolytic crack growth under various other conditions. For example, hydrolysis and transport of active species have different dependence on temperature. Measuring crack velocity at various temperatures may help to understand rate-limiting processes for hydrolytic crack growth. We also hope to observe hydrolytic crack growth in the atmospheric environment, in which both relative humidity and temperature can be varied.

4.4. Ductile to brittle transition

When a sample is strained beyond the yield point, the polymer chains overcome the interchain friction, and slip. If chain slip mediates extensive deformation, the sample is ductile. As chains slip, they may jam by entanglements between the chains. Once jammed, the chains build up tension along themselves. For some thermoplastics, chains disentangle, and the sample fractures by chain slip. For other thermoplastics, the tension in the chains reaches the covalent bond strength, and the sample fractures by chain scission.

When a PET sample with a precut is stretched in air, polymer chains near the crack tip slip due to the stress concentration. With increasing applied load, the plastic zone expands with more chains slipping. As the energy release rate approaches the toughness of the PET, the crack grows with chain scission. When a PET sample with a precut is submerged in an aqueous environment with reactive species, polymer chains break upon a combination of external loading and hydrolysis. Such chain scission takes time. When the crack advances too fast for hydrolysis to take place, chains slip extensively prior to scission, leading to a high energy release rate. When the crack advances slowly enough for hydrolysis to take place, chains slip negligibly prior to scission, leading to a low energy release rate. Consequently, hydrolysis causes a ductile to brittle transition.

4.5. Hydrolytic crack growth in SiO_2

We can compare hydrolytic crack growth in PET and in silica, which has been extensively studied. In studying hydrolytic crack growth in silica, it has been common to use the measured relation between crack velocity and energy release rate (i.e., the v-G curve) to deduce the energetics and kinetics of stress-assisted hydrolysis (Cook and Liniger, 1993; Vlassak et al., 2005). Hydrolytic crack growth in silica shows three regimes of behavior (Ciccotti, 2009). In regime I, where the energy release rate is slightly higher than the threshold, hydrolysis near the crack tip is set by the level of stress concentration, and strained silicon-oxygen bonds lower the activation energy, and accelerate hydrolysis, so that the crack velocity is sensitive to energy release rate. In regime II, at a more elevated energy release rate, hydrolysis is controlled by the transport of water to the crack tip; crack velocity is nearly independent of energy release rate and plateaus. The plateau velocity increases with the relative humidity in air, and disappears when the sample is submerged in water. In regime III, when the energy release rate approaches the toughness, the crack propagates rapidly with negligible hydrolysis.

For hydrolytic crack growth in PET, however, the v-G curve is greatly affected by plastic deformation. Because the plastic deformation associated with crack growth is not fully characterized by itself, the v-G curve cannot be used directly to deduce the energetics and kinetics of stress-assisted hydrolysis. Furthermore, as suggested by the Lake-Thomas model, before a polymer chain breaks, the high stress is transmitted over some length of the polymer chain (Lake et al., 1997). When the polymer chain breaks at a

single atomic bond, the energy stored in some length of the chain is dissipated. For PET, the mechanisms for the observed changes in crack velocity have not yet been studied. Further investigation is needed to understand the threshold of energy release rate below which crack does not grow. It is unknown whether the stress concentration lowers the energy barrier to hydrolysis. The reactive species (i.e., water, hydroxide ions, or hydronium ions) can transport in the surrounding solution, as well as in the polymer. The effects of rates of transport on crack velocity have not been studied. Given these challenges, in this paper, no attempt has been made to deduce the energetic and kinetics of stress-assisted hydrolysis in PET using the v-G curve. This said, the activation energy barrier for hydrolysis of PET in neutral pH in the absence of stress is estimated to be 90 kJ/mol (Golike and Lasoski, 1960).

4.6. Hydrolytic crack growth in poly(lactic acid) (PLA)

Hydrolytic crack growth has recently been studied in a bio-derived and biodegradable polyester: PLA. At a constant energy release rate ($G \approx 200$ J/m^2), the crack velocity varies up to four orders of magnitude between pH = 1 to pH = 12, where the basic environment greatly accelerates crack growth (Shi et al., 2022). The authors demonstrate the trend shows great resemblance with that of the rate of hydrolysis of PLA oligomers in various pH environments.

In the present study of PET, at a high pH, comparable crack velocities are observed at a much higher energy release rate ($G \approx 4{,}400$ J/m^2). For a given crack velocity, the energy release rate is set by both chain scission and chain slip. The contribution of chain scission is sensitive to the chemistry. The contribution of chain slip depends on the interchain friction. PLA and PET have different molecular structures, which may undergo hydrolysis at different rates. The two thermoplastics also have different interchain friction, which may cause different amounts of plastic dissipation. To sort out these contributions, however, requires a much more extensive experimental investigation than reported here. At a low pH, as we noted before, the duration and spatial resolution of our experiments are too narrow for us to observe any crack growth.

Like PET, PLA also undergoes a ductile to brittle transition. When the crack velocity is low and reaction rate is high, chain scission dominates, and the fracture surface is smooth. When the crack velocity is high and the reaction rate is low, chain slip dominates, and the fracture surface shows extensive plastic deformation (Shi et al., 2022).

4.7. Impact on sustainable uses of polymers

Hydrolytic crack growth in PET has not been reported before. This finding is directly relevant to the development of sustainable uses of post-consumer PET. About 65 million tonnes of food packaging plastics are landfilled across the globe (The New Plastics Economy, 2016). In a landfill, a PET bottle has an estimated half life of 2,500 years (Chamas et al., 2020). Since PET is abundant and is not degradable, one strategy to mitigate waste is to reuse post-consumer PET. It is critical to realize the stability of PET in its conventional applications, such as drink bottles and food containers, may be insufficient for repurposed applications. In particular, for any load-bearing applications, the chemomechanical stability of PET must be reevaluated to consider hydrolytic crack growth. For example, recycled PET fibers have been explored as reinforcement for concrete. Adding recycled PET to fresh concrete decreases its weight and increases its workability. It has shown that the addition of PET fibers to concrete leads to increases in flexural toughness and impact resistance after 28 days (Gu and Ozbakkaloglu, 2016). However, the enhancement deteriorates quickly and completely disappears after only 150 days. The authors attributed this short-lived enhancement to the degradation of fibers in concrete, which is highly alkaline (Gu and Ozbakkaloglu, 2016). This observation echoes our finding: load-bearing PET is susceptible to hydrolytic crack growth in wet and basic environments.

Thermomechanical recycling of PET has also long been pursued and has remained a challenge (Schyns and Shaver, 2021). During thermomechanical recycling, the post-consumer PET products are cleaned, ground into flakes, dried, melted, and extruded (Awaja and Pavel, 2005). Scission of polymer chains leads to PET of inferior mechanical behavior, and should be minimized. Scission may be caused by contaminants including water and acid producing products (Webb et al., 2013). It remains to be seen whether thermomechanical recycling of PET is affected by hydrolytic crack growth. Hydrolytic crack growth increases the rate of degradation at crack tips by orders of magnitude, but not the rate of bulk degradation. Independent of whether hydrolytic crack growth affects thermomechanical recycling, our work indicates that one needs to exercise caution when using post-consumer PET in structural applications.

Growing concerns over non-degradable plastic waste has also led to the development of degradable plastics. Degradable plastics are being used for biomedical applications, such as degradable sutures and implants (Chu and Cambell, 1982). Like PLA and PET, many biodegradable polymers and biomass-derived polymers under development have hydrolysable chains. Examples include poly(caprolactone) and poly(hydroxyalkanoate) (Peptu and Kowalczuk, 2018; Sudesh and Iwata, 2008). These polymers with hydrolysable chains are likely vulnerable to hydrolytic crack growth. Polymers in many biomedical applications bear loads, and hydrolytic crack growth should be characterized to prevent premature failure.

5. Concluding remarks

Hydrolytic crack growth is commonly studied in glass and ceramics, in which oxygen bridges are vulnerable to hydrolysis (Ciccotti, 2009; Cook and Liniger, 1993; Vlassak et al., 2005; Wiederhorn, 1967). Most familiar commercial plastics, such as polyethylene, polypropylene, and polyvinyl chloride, consist of carbon chains, which are not vulnerable to hydrolysis. This fact perhaps explains the paucity of literature on hydrolytic crack growth in polymers. By contrast, many biodegradable and bio-derived polymers contain hydrolysable groups in their backbones. As these materials are under development to replace conventional plastics, it is significant to characterize hydrolytic crack growth in polymers containing hydrolysable groups. Among commonly used plastics, PET is special in

that its backbone does contain hydrolysable groups, but hydrolytic crack growth in PET has not been reported in the literature. Given its availability at low cost and the broad processing knowledge, PET may as well function as a model material to study hydrolytic crack growth in polymers.

In summary, we have discovered hydrolytic crack growth in PET in aqueous solutions. Hydrolysis embrittles PET. Given the widespread use of PET, its hydrolytic fracture should be further studied to uncover the molecular processes. In particular, little is known about the transport of active species in PET or the effect of stress on hydrolytic chain scission. Hydrolytic fracture is potentially important for any polymer that contains hydrolysable bonds, either as repeat units in polymer chains, or as crosslinks between polymer chains. PET today is mostly landfilled and takes millennia to degrade. As the combat against plastic waste escalates, innovative uses of post-consumer PET are being explored, some of which require PET to bear loads. Furthermore, biodegradable and biomass-derived polymers are being developed, many of which contain hydrolysable bonds and are intended to replace load-bearing nondegradable, petroleum-derived polymers. In addition to these opportunities for sustainable uses of polymers, degradable and bio-derived polymers are being developed for medical applications. For all these opportunities, it is hoped that the findings of hydrolytic crack growth and embrittlement will inform future development.

CRediT authorship contribution statement

Atte Kadoma: Investigation, Validation, Formal analysis, Visualization, Methodology, Writing – original draft, Writing – review & editing. **Quan Jiao:** Investigation, Software, Supervision, Methodology, Validation, Writing – original draft, Writing – review & editing. **Joost J. Vlassak:** Funding acquisition, Supervision, Methodology, Writing – review & editing. **Zhigang Suo:** Conceptualization, Methodology, Writing – review & editing, Funding acquisition, Supervision.

Declaration of Competing Interest

The authors declare that they have no known competing financial interests or personal relationships that could have appeared to influence the work reported in this paper.

Data availability

Data will be made available on request.

Acknowledgements

This research was supported by the Harvard University MRSEC, which is funded by the National Science Foundation under Grant DMR-2011754. Part of this work was performed at the Center for Nanoscale Systems (CNS), which is supported by the National Science Foundation under Grant ECS 1541959.

References

Allen, N.S., Edge, M., Mohammadian, M., Jones, K., 1994. Physicochemical aspects of the environmental degradation of poly(ethylene terephthalate). Polym. Degrad. Stab. 43, 229–237. https://doi.org/10.1016/0141-3910(94)90074-4.
Amborski, L.E., Flierl, D.W., 1953. Physical properties of polyethylene terephthalate films. Ind. Eng. Chem. 45, 2290–2295. https://doi.org/10.1021/ie50526a042.
Awaja, F., Pavel, D., 2005. Recycling of PET. Eur. Polym. J. 41, 1453–1477. https://doi.org/10.1016/j.eurpolymj.2005.02.005.
Baumberger, T., 2022. Hydrolytic embrittlement: A security breach in structural materials made of biodegradable polymers. MRS Bull. https://doi.org/10.1557/s43577-022-00421-3.
Braden, M., Gent, A.N., 1960. The attack of ozone on stretched rubber vulcanizates. I. The rate of cut growth. J. Appl. Polym. Sci. 3, 90–99. https://doi.org/10.1002/app.1960.070030713.
Burkersroda, F.von, Schedl, L., Göpferich, A., 2002. Why degradable polymers undergo surface erosion or bulk erosion. Biomaterials 23, 4221–4231. https://doi.org/10.1016/S0142-9612(02)00170-9.
Buxbaum, L.H., 1968. The degradation of poly(ethylene terephthalate). Angew. Chem. Int. Ed. Engl. 7, 182–190. https://doi.org/10.1002/anie.196801821.
Chamas, A., Moon, H., Zheng, J., Qiu, Y., Tabassum, T., Jang, J.H., Abu-Omar, M., Scott, S.L., Suh, S., 2020. Degradation rates of plastics in the environment. ACS Sustain. Chem. Eng. 8, 3494–3511. https://doi.org/10.1021/acssuschemeng.9b06635.
Chen, C., Wang, Z., Suo, Z., 2017. Flaw sensitivity of highly stretchable materials. Extreme Mech. Lett., Filling Gaps in Material Property Space: IUTAM Symposium 10, 50–57. https://doi.org/10.1016/j.eml.2016.10.002.
Chu, C.C., Campbell, N.D., 1982. Scanning electron microscopic study of the hydrolytic degradation of poly(glycolic acid) suture. J. Biomed. Mater. Res. 16, 417–430. https://doi.org/10.1002/jbm.820160410.
Ciccotti, M., 2009. Stress-corrosion mechanisms in silicate glasses. J. Phys. Appl. Phys. 42, 214006 https://doi.org/10.1088/0022-3727/42/21/214006.
Cook, R.F., Liniger, E.G., 1993. Kinetics of indentation cracking in glass. J. Am. Ceram. Soc. 76, 1096–1105. https://doi.org/10.1111/j.1151-2916.1993.tb03726.x.
De Falco, F., Di Pace, E., Cocca, M., Avella, M., 2019. The contribution of washing processes of synthetic clothes to microplastic pollution. Sci. Rep. 9, 6633. https://doi.org/10.1038/s41598-019-43023-x.
Geyer, R., Jambeck, J.R., Law, K.L., 2017. Production, use, and fate of all plastics ever made. Sci. Adv. 3, e1700782 https://doi.org/10.1126/sciadv.1700782.
Golike, R.C., Lasoski, S.W., 1960. Kinetics of hydrolysis of polyethylene terephthalate films. J. Phys. Chem. 64, 895–898. https://doi.org/10.1021/j100836a018.
Göpferich, A., 1996. Mechanisms of polymer degradation and erosion. In: Williams, D.F. (Ed.), The Biomaterials: Silver Jubilee Compendium. Elsevier Science, Oxford, pp. 117–128. https://doi.org/10.1016/B978-008045154-1.50016-2.
Griffith, A.A., Taylor, G.I., 1921. VI. The phenomena of rupture and flow in solids. Philos. Trans. R. Soc. Lond. Ser. Contain. Pap. Math. Phys. Character 221, 163–198. https://doi.org/10.1098/rsta.1921.0006.
Gu, L., Ozbakkaloglu, T., 2016. Use of recycled plastics in concrete: a critical review. Waste Manag 51, 19–42. https://doi.org/10.1016/j.wasman.2016.03.005.

Hosseini, S.S., Taheri, S., Zadhoush, A., Mehrabani-Zeinabad, A., 2007. Hydrolytic degradation of poly(ethylene terephthalate). J. Appl. Polym. Sci. 103, 2304–2309. https://doi.org/10.1002/app.24142.
Hunt, C.F., Lin, W.H., Voulvoulis, N., 2021. Evaluating alternatives to plastic microbeads in cosmetics. Nat. Sustain. 4, 366–372. https://doi.org/10.1038/s41893-020-00651-w.
Jia, Y., Zhou, Z., Jiang, H., Liu, Z., 2022. Characterization of fracture toughness and damage zone of double network hydrogels. J. Mech. Phys. Solids 169, 105090. https://doi.org/10.1016/j.jmps.2022.105090.
Jiao, Q., Shi, M., Yin, T., Suo, Z., Vlassak, J.J., 2021. Composites retard hydrolytic crack growth. Extreme Mech. Lett. 48, 101433 https://doi.org/10.1016/j.eml.2021.101433.
Jung, J.H., Ree, M., Kim, H., 2006. Acid- and base-catalyzed hydrolyses of aliphatic polycarbonates and polyesters. Catal. Today. In: Proceedings of the 8th International Conference on Carbon Dioxide Utilization, 115, pp. 283–287. https://doi.org/10.1016/j.cattod.2006.02.060.
Kaabel, S., Therien, J.P.D., Deschênes, C.E., Duncan, D., Friščić, T., Auclair, K., 2021. Enzymatic depolymerization of highly crystalline polyethylene terephthalate enabled in moist-solid reaction mixtures. Proc. Natl. Acad. Sci. 118 https://doi.org/10.1073/pnas.2026452118 e2026452118.
Kothari, V.K., Deopura, B.L., Alagirusamy, R., Joshi, M., 2008. 14 - Polyester and polyamide fibres – apparel applications. In: Gupta, B. (Ed.), Polyesters and Polyamides, Woodhead Publishing Series in Textiles. Woodhead Publishing, pp. 419–440. https://doi.org/10.1533/9781845694609.3.419.
Lake, G.J., Thomas, A.G., Tabor, D., 1997. The strength of highly elastic materials. Proc. R. Soc. Lond. Ser. Math. Phys. Sci. 300, 108–119. https://doi.org/10.1098/rspa.1967.0160.
Lim, X., 2021. Microplastics are everywhere — but are they harmful? Nature 593, 22–25. https://doi.org/10.1038/d41586-021-01143-3.
Lu, M., Huang, S., Chen, S., Ju, Q., Xiao, M., Peng, X., Wang, S., Meng, Y., 2018. Transparent and super-gas-barrier PET film with surface coated by a polyelectrolyte and Borax. Polym. J. 50, 239–250. https://doi.org/10.1038/s41428-017-0015-5.
McMahon, W., Birdsall, H.A., Johnson, G.R., Camilli, C.T., 1959. Degradation studies of polyethylene terephthalate. J. Chem. Eng. Data 4, 57–79. https://doi.org/10.1021/je60001a009.
Militky, J., 2009. The chemistry, manufacture and tensile behaviour of polyester fibers. Handbook of Tensile Properties of Textile and Technical Fibres. Elsevier, pp. 223–314. https://doi.org/10.1533/9781845696801.2.223.
Nisticò, R., 2020. Polyethylene terephthalate (PET) in the packaging industry. Polym. Test. 90, 106707 https://doi.org/10.1016/j.polymertesting.2020.106707.
Orowan, E., 1944. The fatigue of glass under stress. Nature 154, 341–343. https://doi.org/10.1038/154341a0.
Peptu, C., Kowalczuk, M., 2018. 8 - biomass-derived polyhydroxyalkanoates: biomedical applications. In: Popa, V., Volf, I. (Eds.), Biomass as Renewable Raw Material to Obtain Bioproducts of High-Tech Value. Elsevier, pp. 271–313. https://doi.org/10.1016/B978-0-444-63774-1.00008-9.
Proctor, B.A., Whitney, I., Johnson, J.W., Cottrell, A.H., 1997. The strength of fused silica. Proc. R. Soc. Lond. Ser. Math. Phys. Sci. 297, 534–557. https://doi.org/10.1098/rspa.1967.0085.
Ragaert, K., Delva, L., Van Geem, K., 2017. Mechanical and chemical recycling of solid plastic waste. Waste Manag 69, 24–58. https://doi.org/10.1016/j.wasman.2017.07.044.
Ravens, D.A.S., 1960. The chemical reactivity of poly(ethylene terephthalate): Heterogeneous hvdrolysis by hydrochloric acid. Polymer 1, 375–383. https://doi.org/10.1016/0032-3861(60)90047-1.
Rivlin, R.S., Thomas, A.G., 1953. Rupture of rubber. I. Characteristic energy for tearing. J. Polym. Sci. 10, 291–318. https://doi.org/10.1002/pol.1953.120100303.
Robertson, G.L., 2016. Food Packaging: Principles and Practice, Third Edition. CRC Press.
Ronkay, F., Molnár, B., Nagy, D., Szarka, G., Iván, B., Kristály, F., Mertinger, V., Bocz, K., 2020. Melting temperature versus crystallinity: new way for identification and analysis of multiple endotherms of poly(ethylene terephthalate). J. Polym. Res. 27, 372. https://doi.org/10.1007/s10965-020-02327-7.
Ronkvist, Å.M., Xie, W., Lu, W., Gross, R.A., 2010. Surprisingly rapid enzymatic hydrolysis of poly(ethylene terephthalate). Green Polymer Chemistry: Biocatalysis and Biomaterials, ACS Symposium Series. American Chemical Society, pp. 385–404. https://doi.org/10.1021/bk-2010-1043.ch026.
Rytöluoto, I., Gitsas, A., Pasanen, S., Lahti, K., 2017. Effect of film structure and morphology on the dielectric breakdown characteristics of cast and biaxially oriented polypropylene films. Eur. Polym. J. 95, 606–624. https://doi.org/10.1016/j.eurpolymj.2017.08.051.
Schyns, Z.O.G., Shaver, M.P., 2021. Mechanical recycling of packaging plastics: a review. Macromol. Rapid Commun. 42, 2000415 https://doi.org/10.1002/marc.202000415.
Sevim, K., Pan, J., 2018. A model for hydrolytic degradation and erosion of biodegradable polymers. Acta Biomater 66, 192–199. https://doi.org/10.1016/j.actbio.2017.11.023.
Shayanipour, H.R., Bagheri, R., 2019. Barrier improvement of the biaxial oriented polypropylene films using passive mechanisms. J. Mater. Res. Technol. 8, 2987–2995. https://doi.org/10.1016/j.jmrt.2017.06.012.
Shi, M., Jiao, Q., Yin, T., Vlassak, J.J., Suo, Z., 2022. Hydrolysis embrittles poly(lactic acid). MRS Bull. https://doi.org/10.1557/s43577-022-00368-5.
Shi, M., Steck, J., Yang, X., Zhang, G., Yin, J., Suo, Z., 2020. Cracks outrun erosion in degradable polymers. Extreme Mech. Lett. 40, 100978 https://doi.org/10.1016/j.eml.2020.100978.
Sudesh, K., Iwata, T., 2008. Sustainability of biobased and biodegradable plastics. CLEAN – Soil Air Water 36, 433–442. https://doi.org/10.1002/clen.200700183.
The future of plastic, 2018. Nat. Commun. 9, 2157. 10.1038/s41467-018-04565-2.
The New Plastics Economy: Rethinking the future of plastics [WWW Document], 2016. URL https://ellenmacarthurfoundation.org/the-new-plastics-economy-rethinking-the-future-of-plastics (accessed 1.31.23).
Tian, Z., Zhao, H., Peter, K.T., Gonzalez, M., Wetzel, J., Wu, C., Hu, X., Prat, J., Mudrock, E., Hettinger, R., Cortina, A.E., Biswas, R.G., Kock, F.V.C., Soong, R., Jenne, A., Du, B., Hou, F., He, H., Lundeen, R., Gilbreath, A., Sutton, R., Scholz, N.L., Davis, J.W., Dodd, M.C., Simpson, A., McIntyre, J.K., Kolodziej, E.P., 2021. A ubiquitous tire rubber–derived chemical induces acute mortality in coho salmon. Science 371, 185–189. https://doi.org/10.1126/science.abd6951.
Vlassak, J.J., Lin, Y., Tsui, T.Y., 2005. Fracture of organosilicate glass thin films: environmental effects. Mater. Sci. Eng. A 391, 159–174. https://doi.org/10.1016/j.msea.2004.08.070.
Webb, H.K., Arnott, J., Crawford, R.J., Ivanova, E.P., 2013. Plastic degradation and its environmental implications with special reference to poly(ethylene terephthalate). Polymers 5, 1–18. https://doi.org/10.3390/polym5010001.
Wiederhorn, S.M., 1968. Moisture assisted crack growth in ceramics. Int. J. Fract. Mech. 4, 171–177. https://doi.org/10.1007/BF00188945.
Wiederhorn, S.M., 1967. Influence of water vapor on crack propagation in soda-lime glass. J. Am. Ceram. Soc. 50, 407–414. https://doi.org/10.1111/j.1151-2916.1967.tb15145.x.
Yang, X., Steck, J., Yang, J., Wang, Y., Suo, Z., 2021. Degradable plastics are vulnerable to cracks. Engineering 7, 624–629. https://doi.org/10.1016/j.eng.2021.02.009.
Yang, X., Yang, J., Chen, L., Suo, Z., 2019. Hydrolytic crack in a rubbery network. Extreme Mech. Lett. 31, 100531 https://doi.org/10.1016/j.eml.2019.100531.